Turk J Phys
27 (2003) , 419 – 426.

Au Nanoparticle Clusters: A New System to Model Hopping Conduction

Ç. KURDAK, J. KIM, L. A. FARINA, K. M. LEWIS, X. BAI
Department of Physics, University of Michigan, Ann Arbor, MI 48109, USA
M. P. ROWE, A. J. MATZGER
Department of Chemistry, University of Michigan, Ann Arbor, MI 48109, USA

Received 28.08.2003

Abstract

We study electrical transport through self-assembled Au nanoparticle clusters which can be viewed as a new model system to study hopping transport. The physics of such systems is governed by two parameters: the charging energy and tunnel coupling between the particles. The charging energy is determined by the size of the nanoparticles. When the diameter of the nanoparticles is less than 4-5 nm the charging energy is large enough that Coulomb blockade effects were observed in electrical transport even at room temperature. The magnitude of the tunnel coupling between the particles was determined by the thiol coating used. To study a wide range of tunnel couplings, we have synthesized gold nanoparticles with various thiol coatings, including 1-octanethiol, 1-dodecanethiol, 1-octadecanethiol, 4-mercaptodiphenylacetylene, 4-nitro-4-mercaptodiphenylacetylene, and 3,5-dinitro-4-mercaptodiphenylacetylene. Current-voltage characteristics were found to be strongly dependent on both the coating and the size of the nanoparticles. At low temperature we have observed nonlinear I-V characteristics with a threshold voltage that was significantly larger in gold nanoparticle clusters where the thiol coating had weak tunnel coupling.

Key Words: nanoparticles, Coulomb blockade, hopping conduction.

1. Introduction

Metallic and superconductor islands linked by tunnel junctions have long been used as model systems to study a rich variety of physical phenomena[1]. The physics of such systems are governed mainly by two parameters: the charging energy of the islands which is determined by the capacitance of the islands and the tunnel coupling between the islands which is determined by tunnel resistance between the islands. For studying lower-dimensional phenomena, systems of $Al/AlO_x/Al$ tunnel junctions have been shown to be extremely versatile since both the resistance and the tunnel capacitance of such junctions can be engineered by fabrication. Using this material system, systems of single or few islands[2, 3] as well as arrays of one- and two-dimensional islands, have already been studied[4, 5, 6, 7, 8]. The islands that are defined lithographically have typical dimensions of around 1 micron and the tunnel junctions are about 0.001-0.01 μm^2. The large size of the islands requires the experiments to be carried out at dilution refrigerator temperatures.

Lithographical techniques, however, are not suitable for creating systems to model three-dimensional phenomena. Recently, a new approach has emerged to realize two- and three-dimensional systems of coupled islands based on self-assembly of Au nanoparticles[9, 10, 11, 12, 13]. In this approach the islands are not defined lithographically; instead, they are synthesized by various chemical techniques. Correspondingly, the sizes of the particles are sufficiently small that single electron effects are observable even at room temperature. With the thiol coatings currently being used, the tunnel coupling between the nanoparticles is much smaller

than that of $Al/AlO_x/Al$ tunnel junctions. Thus, the system of Au nanoparticle clusters enable us to cover a parameter space that is not accessible by lithographically defined tunnel junctions. The parameter spaces that have been covered by these two complementary systems are shown in Fig. 1. In this paper, we will present transport measurements obtained from highly disordered Au nanoparticle clusters which are well suited to model hopping transport in three dimensions.

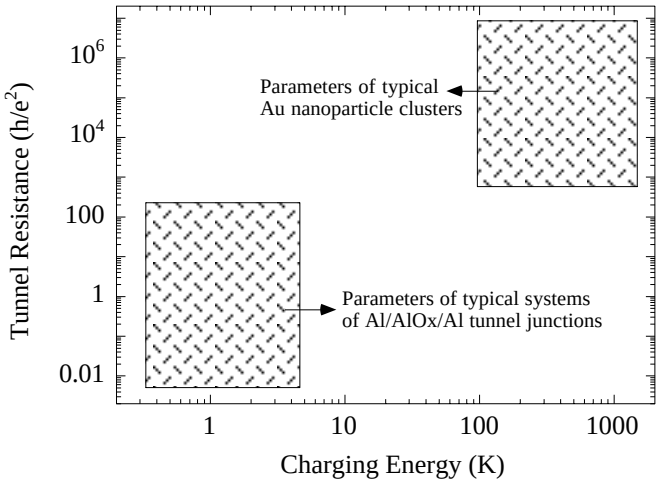

Figure 1. The parameter spaces that are covered by $Al/AlO_x/Al$ tunnel junctions and systems of coupled Au nanoparticles.

In addition to being used as model systems to study physical phenomena, metal nanoparticles have also been viewed as a potential building block for nanoelectronics applications. More recently, Au nanoparticle clusters have attracted interest as they can be used as highly sensitive chemosensors to detect volatile organic chemicals[14]. A fundamental understanding of electrical transport through such metal nanoparticle clusters is essential for progress in such applications.

2. Synthesis of Au Nanoparticles

Synthesis of a variety of Au nanoparticles with different coatings are needed to model a wide range of physical phenomena. Motivated by the limitations of the published nanoparticle synthesis methods, we have developed a strategy that would accommodate a broad range of ligands, similar to the Brust reaction[15], but which does not need a phase transfer catalyst to produce gold nanoparticles. The general procedure of the Au nanoparticle synthesis is illustrated in Fig. 2. Hydrogen tetrachloroaurate is dissolved in anhydrous tetrahydrofuran (THF). The desired ligand is then added to this solution. The core size of synthesized nanoparticle can be controlled at this point by varying the number of equivalents of thiol used with respect to the gold salt. Lithium borohydride is added followed by addition of toluene and removal of the tetrahydrofuran under reduced pressure. The gold nanoparticles solution is further diluted with toluene and washed with water to remove any reducing agent byproducts. The toluene is then removed and the crude product is collected on a fritted glass funnel and washed with acetonitrile and ethanol[16]. The purified gold nanoparticles are collected with toluene to form a stable colloidal suspension.

This procedure has proven to be a very versatile means for production of pure gold nanoparticles that are free of any ionic species capable of interfering with electronic measurements. Examples of products include the gold nanoparticles capped with 1-octanethiol (C8), 1-dodecanethiol (C12), 1-octadecanethiol (C18), 4-mercaptodiphenylacetylene (DPA), 4-nitro-4-mercaptodiphenylacetylene (NDPA), and 3,5-dinitro-4-mercaptodiphenylacetylene (DNDPA). Sizewise this synthetic method reliably produces quite monodisperse nanoparticles. The average core size and the size dispersion of the nanoparticles were determined

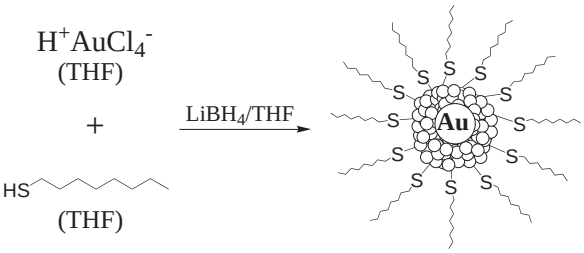

Figure 2. Reaction scheme of the homogeneous organic phase nanoparticle synthesis method.

using TEM studies. A TEM image and a histogram of gold nanoparticle diameters prepared with this method are shown in Fig. 3.

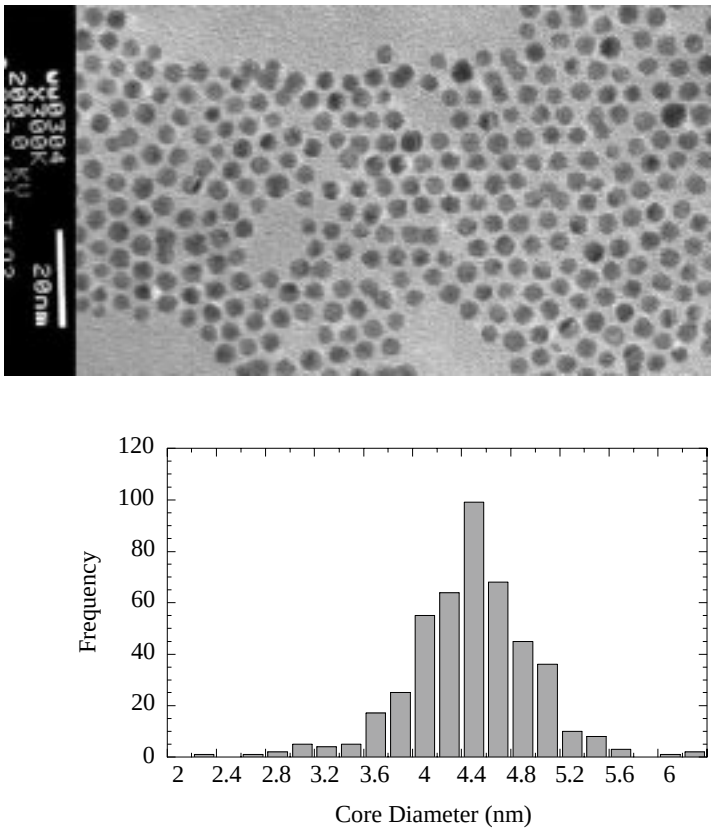

Figure 3. TEM image of C8 coated Au nanoparticles synthesized using the above procedure and the corresponding histogram of Au nanoparticle diameters.

A more detailed description of the Au nanoparticle synthesis process will be published elsewhere[17].

3. Electrical Measurements

In most cases, due to the very high resistance of the Au nanoparticle films, interdigitated electrodes are needed to study transport properties of such films. 20 nm tall Au interdigitated electrodes with 50 fingers, with a finger length of 9 μm and electrode spacing of 100 nm, were fabricated on an insulating silicon oxide

film by electron beam lithography. A SEM picture of the interdigitated electrode structure used in our experiments is shown in Fig. 4.

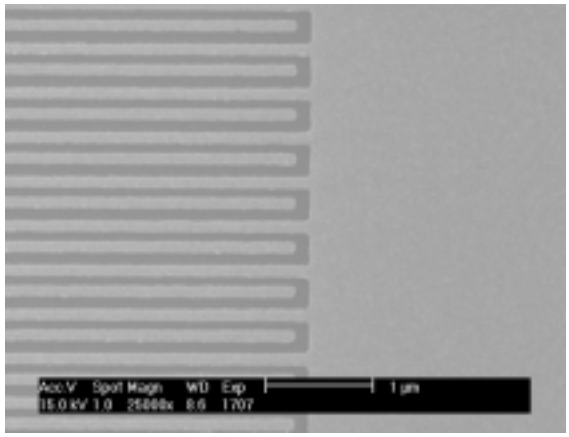

Figure 4. Interdigitated electrodes with 100 nm spacing fabricated using electron-beam lithography.

Au nanoparticles that were suspended in toluene are deposited on such interdigitated electrodes using an airbrush technique. The films prepared by this technique are found to be highly nonuniform in thickness. In the first few hours after the deposition of the nanoparticles the film resistance is found to be changing due to toluene evaporation. All electrical measurements were performed after the films were fully dry, typically 1-2 days after the deposition of the films.

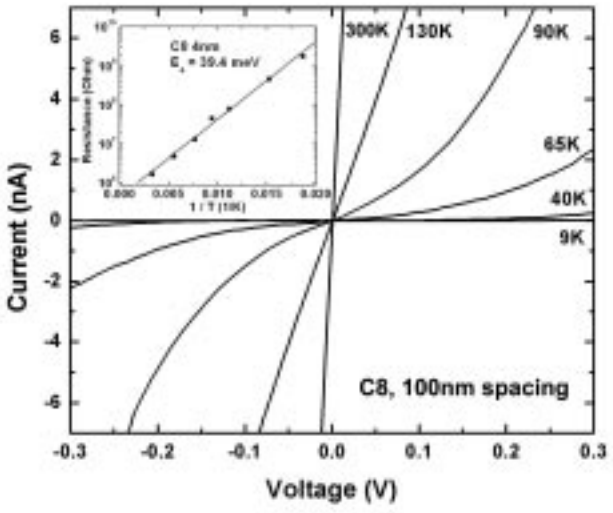

Figure 5. I-V characteristics of a 4 nm diameter C8 coated Au nanoparticle film at different temperatures. The inset shows the small-bias resistance of the film as a function of inverse temperature where the solid line is a fit to an Arrhenius exponential form.

Current-voltage measurements were performed on a wide range of nanoparticle films, in a variable temperature cryostat from room temperature down to 1.5 K. All the films that we have studied exhibit nonlinear I-V characteristics and insulating behavior at low temperatures. Typical I-V characteristics obtained from a thin film consisting of 4.3 nm size Au nanoparticles coated with C8 are shown in Fig. 5. The insulating behavior is evident in the non-linear I-V characteristics at low temperatures as well as the temperature

dependence of the small-bias resistance. The small-bias resistance is found to be thermally activated with an activation energy of 39 meV as shown in the inset of Fig 5. The insulating behavior arises from the single electron effects; as the size of the particles becomes sufficiently small there is charging energy associated with electron tunneling which can be larger than thermal energy and thus tunneling is not allowed at low temperatures[18]. The size of the charging energy is given by $e^2/2C$ where C is the island capacitance. In real systems, there are trapped charges near the nanoparticles which would lead to a random offset charge disorder. In the presence of such disorder, current does not flow uniformly through the nanoparticle film. In fact it is possible that there may be a few energetically favorable paths that carry most of the current[19, 20]. Because of such kind of disorder, the charging energy extracted from the temperature dependent data is always smaller that the charging energy[21].

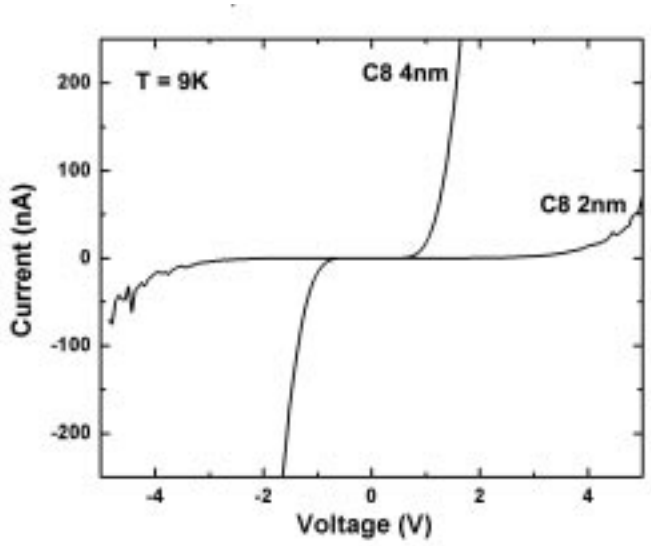

Figure 6. I-V characteristics of 2.2 nm and 4.3 nm diameter C8 coated Au nanoparticle films at T = 1.5 K.

The magnitude of the charging energy can be engineered by changing the size of the nanoparticles. To test this idea, we synthesized Au nanoparticles of different sizes. The I-V characteristics of films made from 2.2 nm and 4.3 nm diameter Au nanoparticles are shown in Fig 6. As expected, the film made with 2.2 nm diameter Au nanoparticles is found to exhibit a larger Coulomb gap in the I-V characteristics. The charging energy for 2.2 nm diameter Au nanoparticles is much larger than the thermal energy at room temperature. In fact, the small bias resistance of this film was unmeasurably large even at room temperature, consistent with a large Coulomb gap. In principle the size of the charging energy can also be engineered by changing the dielectric constant of the medium between the nanoparticles.

In addition to charging energy we must also be able to engineer the tunnel coupling between the islands. There are two strategies to engineer the tunnel coupling. The first strategy is to change the distance between the nanoparticles by using different sized thiol coatings. The second strategy is to control the energy barrier for tunneling. For tunneling of electrons the relevant energy barrier is given by the energy of the lowest unoccupied molecular orbitals (LUMO) of the thiol coating. To test these ideas we have synthesized Au nanoparticles with various coatings that had an approximate core diameter of 3-5 nm. These Au nanoparticle films showed activated behavior with activation energies ranging from 26-45 meV. The I-V characteristics of three Au nanoparticle films with different sized thiol coatings, C8, C12, and C18, are shown in Fig. 7. The energies of the LUMOs for these three alkyl chains are expected to be similar. Thus, a difference in transport properties for these films is expected to arise from the different tunnel coupling. The trend from lowest to highest resistance for alkylthiol coated Au nanoparticles films is C8, C12, then C18, with C18 being immeasurably high. This is consistent with the thicker thiol coatings forming more resistive films. The second strategy is to control tunnel coupling by using thiol coatings with LUMOs with different energies. It is well known that there are conjugated ligands that have LUMO energies that are lower than that of alkyl chains. Au nanoparticles coated with such ligands are expected to have stronger tunnel coupling. I-V characteristics

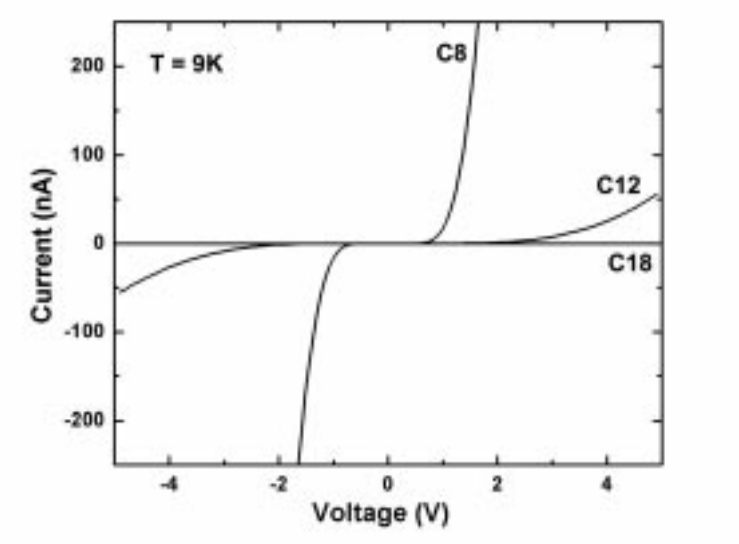

Figure 7. I-V characteristics of C8, C12, and C18 coated Au nanoparticle films at T=9 K. The average diameters of the nanoparticles were 4.3 nm, 4.2 nm, and 3.8 nm, respectively.

of three Au nanoparticle films with similar length but different type of coatings (C12, DNDPA, and NDPA) are shown in Fig. 8. Among these three, the Au nanoparticle film made with C12 coated particles has the largest tunnel resistance, consistent with the highest energy of LUMO for this coating. In short, both strategies seem to be effective in controlling the tunnel coupling between the nanoparticles.

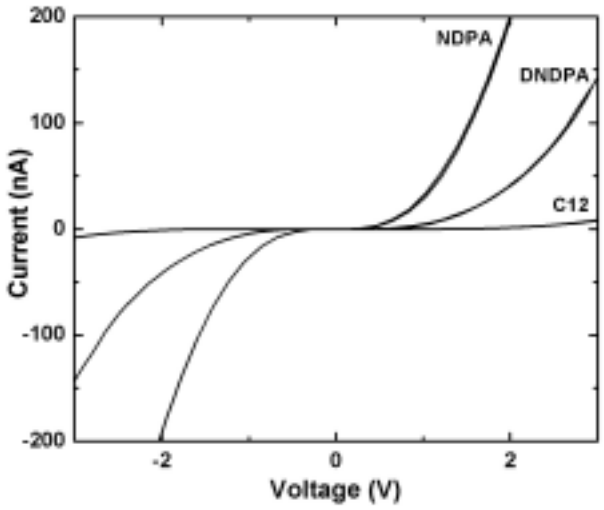

Figure 8. I-V characteristics of C12, NDPA, and DNDPA coated Au nanoparticle films at T=1.5 K. The average diameters of the nanoparticles were 4.2 nm, 3.7 nm, and 3.0 nm, respectively.

4. Conclusions

We view Au nanoparticle clusters as an artificial solid where both the tunnel coupling and the charging energy can be engineered. When a single island or a few islands are involved, the electrical properties can be understood in the frame work of so called "orthodox theory"[18]. However, transport through Au

nanoparticle films is much more complicated and not well understood. In all realistic systems of coupled islands, islands are subject to random offset charges. Numerical simulations performed in two dimensional arrays of metallic islands in the presence of random offset charges indicate that there is a threshold voltage for current flow at zero temperature[19, 20]. For bias voltages greater than the threshold voltage the current is predicted to flow in a few channels. Middleton and Wingreen predicted for two-dimensional arrays of islands a universal I-V characteristic in a regime where the islands have a large self capacitance[19]. Most of the films that we have studied also exhibit Middleton-Wingreen type I-V behavior, $I \propto (V - V_{th})^{\zeta}$, at low temperatures with a scaling exponent of $\zeta \approx 3 \pm 0.8$. The size of the threshold voltage extracted from such fits is found to be significantly larger in gold nanoparticle clusters where the thiol coating has weak tunnel coupling. This is an unexpected result in that the threshold voltage for an array of metal islands should only depend only on the size of the nanoparticles. We believe in addition to offset charges, variations in tunnel couplings between adjacent islands also play an important role in such systems. It is possible that a wide variation in tunnel coupling, could lead to highly meandering paths for current flow. The threshold voltage would depend on the total length of the meandering path which can be much larger than the spacing between the electrodes. Understanding transport in the presence of exponentially wide range of tunnel couplings is relevant to other hopping systems, such as hopping transport in nondegenerate semiconductors and low temperature transport in amorphous materials.

It is important to note that the tunnel couplings that are achieved so far are all in the weak coupling limit, where the tunnel resistance between the islands are always much larger than the quantum resistance of h/e^2. To model quantum transport using Au nanoparticle systems, we need to synthesize Au nanoparticles with shorter ligands having lower energy LUMOs.

Acknowledgements

We thank Ted Zellers, Len Sander, and Brad Orr for many useful discussions, and Katherine E. Plass for performing the TEM imaging. This work is supported by the Alfred P. Sloan Foundation by the NSF through Grant No. DMR-0092726 and DMR-9871177, and by the Engineering Research Center Program of the NSF under Award No. ERC-9986866.

References

[1] H. Grabet, M. Deverot (Eds.), *Single Charge Tunneling, Coulomb Blockade Phenomena in Nanostructures* (NATO ASI, Vol. 294, Plenum Press, New York, 1992).

[2] D. Averin, K.K. Likharev, *J. Low Temp. Phys.*, **62**, (1986), 345.

[3] L.J. Geerligs, V.F. Anderegg, J. Romijn, and J.E. Mooij, *Phys. Rev. Lett.*, **65**, (1990), 377.

[4] B.J. van Wees, H.S.J. van der Zant, and J.E. Mooij, *Phys. Rev. B*, **35**, (1987), 7291.

[5] T.S. Tighe, A.T. Johnson, and M. Tinkham, *Phys. Rev. B*, **44**, (1991), 10286.

[6] A. Kanda, S. Katsumoto, F. Komori, and S. Kobayashi, *J. Phys. Soc. Japan*, **61**, (1992), 1871.

[7] H.S.J. van der Zant, W.J. Elion, L.J. Geerlings, and J.E. Mooij, *Phys. Rev. B*, **54**, (1996), 10081.

[8] P. Delsing C.D. Chen, D.B. Haviland, Y. Harada, and T. Claeson, *Phys. Rev. B*, **50**, (1994), 3959.

[9] M.G. Ancona, W. Kruppa, R.W. Rendell, A.W. Snow, D. Park, and J.B. Boss, *Phys. Rev. B*, **64**, (2001), 033408.

[10] R. Parthasarathy, X.-M. Lin, and H.J. Jaeger, *Phys. Rev. Lett.*, **87**, (2001), 186807.

[11] X.M. Lin, H.M. Jaeger, C.M. Sorenson, and K.J. Klabunde, *J. Phys. Chem. B*, **105**, (2001), 3353.

[12] K.-M. Muller, J. Herrmann, B. Raguse, G. Baxter, and T. Reda, *Phys. Rev. B*, **66**, (2002), 075417.

[13] P.-E. Trudeau, A. Orozco, E. Kwan, and A.-A. Dhirani, *J. Chem. Phys.*, **117**, (2002), 3978.

[14] H. Wohltjen and A.W. Snow, *Anal. Chem.*, **70**, (1998), 2856.

[15] M. Brust, M. Walker, D. Bethell, D.J. Schiffrin, and R. Whyman, *J. Chem. Soc., Chem. Commun.,* (1994), 801.

[16] Y.S. Shon, C. Mazzitelli, and R.W. Murray, *Langmuir*, **17**, (2001), 7735.

[17] M.P. Rowe, K.E. Plass, K. Kibum, E.T. Zellers, A.J. Matzger, *in preparation.*

[18] D.V. Averin and K.K. Likharev, *in Mesoscopic Phenomena in Solids*, edited by B. Altshuler, P. Lee, and R. Webb (North-Holland, Amsterdam, 1991).

[19] A. Alan Middleton and Ned S. Wingreen, *Phys. Rev. Lett.*, **71**, (1993), 3198.

[20] C. Reichhardt and C.J. Olson Reichhardt, *Phys. Rev. Lett.*, **90**, (2002), 046802.

[21] Ç. Kurdak, A.J. Rimberg, T.R. Ho, and J. Clarke, *Phys. Rev B*, **57**, (1998), R6842.